Supplementary Information section

On the different experimental manifestations of two-state “induced fit"- binding of drugs to their cellular targets.

Running title: Exploring “induced fit"-type drug binding.

Georges Vauquelin[1], Isabelle Van Liefde[1] and David C. Swinney[2]

[1] Department Molecular and Biochemical Pharmacology, Vrije Universiteit Brussel, Pleinlaan 2, B-1050 Brussels, Belgium.

[2] Institute for Rare and Neglected Diseases Drug Discovery, 897 Independence Ave, Suite 2C, Mountain View, CA 94043, USA.

Table of Contents

A) Differential equations for different assay conditions

Simulations are based on theoretical models such as in Figures 1b and 6a in the main article. Peculiar to those simulations is that they are entirely based on repeatedly, simultaneously solving the differential equations (listed in Table 1 below) that govern the time-wise changes in target site occupancy over very small time intervals till the desired time point is attained, such as previously described (Vauquelin et al., 2001a). Compared to simulations that rely on equations in where part of the different equations are already replaced by their integrated outcome (such as K_D values in case of bimolecular interactions, Strickland et al., 1975; Hoare et al., 2007; Tummino et al., 2008), the present strategy allows a non-compromised exploration of hemi-equilibrium situations and easily accomodates further refinements of the experimental design.

Table 1

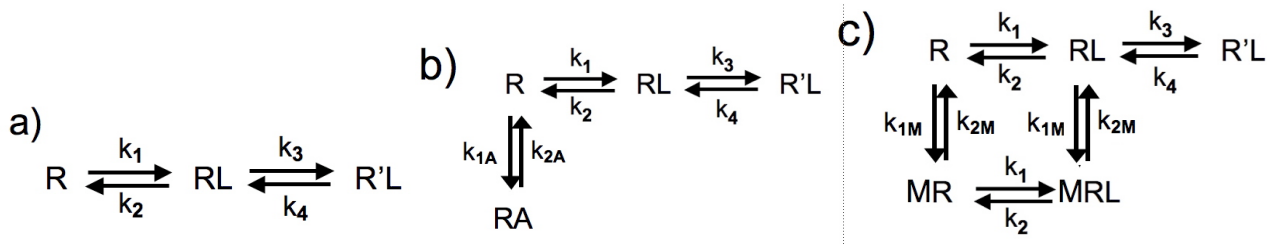

Equations for a:

$$d[R]/d(t) = k_2.[RL] - k_1.[L].[R] \quad \{1\}$$

$$d[RL]/d(t) = k_1.[L].[R] - k_2.[RL] + k_4.[R'L] - k_3.[RL] \quad \{2\}$$

$$d[R'L]/d(t) = k_3 . [RL] - k_4 . [R'L] \quad \{3\}$$

Equations for b (Figure 2 in main article):

keep {2} and {3}, add {4} and replace {1} by {5}

$$d[RA]/d(t) = k_{1A}.[A].[R] - k_{2A}.[RA] \quad \{4\}$$

$$d[R]/d(t) = k_2.[RL] - k_1.[L].[R] + k_{2A}.[RA] - k_{1A}.[A].[R] \quad \{5\}$$

Equations for c (Figure 6 in main article):

keep {3}, add {6} and {7}, replace {1} by {8}and {2} by {9}

$$d[MR]/d(t) = k_{1M}.[M].[R] - k_{2M}.[MR] + k_2.[MRL] - k_1.[L].[MR] \quad \{6\}$$

$$d[MRL]/d(t) = k_{1M}.[M].[RL] - k_{2M}.[MRL] + k_1.[L].[MR] - k_2.[MRL] \quad \{7\}$$

$$d[R]/d(t) = k_2.[RL] - k_1.[L].[R] + k_{2M}.[MR] - k_{1M}.[M].[R] \quad \{8\}$$

$$d[RL]/d(t) = k_1.[L].[R] - k_2.[RL] + k_4.[R'L] - k_3.[RL] + k_{2M}.[MRL] - k_{1M}.[M].[RL] \quad \{9\}$$

Legend to Table 1

a) Induced fit model in where such bimolecular binding is followed by an isomerisation of the initial RL complex into a more stable R'L complex

b) A is an agonist. Its binding R is a reversible bimolecular processes (such as for L in Figure 1a in the main article) and competitive with the binding of L.

c) Binding of M to R and RL are reversible bimolecular processes. In contrast to A, binding of L does not affect binding of M and vice versa. On the other hand, M does not bind to R'L but prevents the isomerisation/conversion of RL into R'L. Such model has already been explored for a situation in where M is a monovalent ligand that only binds to one of the target sites of a heterobivalent ligand (Vauquelin and Charlton, 2013; Vauquelin et al., 2015).

Values of the microkinetic rate constants of each ligand are given in the legends to the figures in the main article.

B) Definitions and values of binding parameters of the investigated L variants (Table 2)

The "thermodynamic" equilibrium dissociation constant $K_D = (k_2.k_4)/(k_1.k_3)$. K_D refers to the difference in Gibbs free energy between the ground state R and the final R'L state as $\Delta G_0 = -RT\ln K_D$ in where R the ideal gas constant and T is temperature in degrees Kelvin.

According to settings the listed in the "Constants, equations and simulations" section of the main article, the reverse isomerisation constant $k_4 = K_D.k_1.k_3 /k_2$

K_D* Stands for [L] at which this observed binding is half maximal at equilibrium. K_D* acts as a "macroscopic" pseudo-binding "affinity" constant and, since both RL and R'L participate in the binding process, it is defined as $K_D^* = k_2.k_4/(k_1.(k_3 + k_4))$.

$^{app}K_D$* Stands for [L] at which the observed binding is half maximal under non-equilibrium conditions. The rationale thereto is that unrealistically long incubation times are needed for the binding of all the investigated L variants to reach binding equilibrium (see Figure 1 below). The present $^{app}K_D$* values were calculated from saturation binding curves after 1 h incubation.

k_2 - k_3 Combinations are disposed in Table 2 according to grid shown in Figure 1e of the main article.

Table 2

	k_2 (min^{-1})	4	1	0.25	0.064	0.016
	k_3 (min^{-1})					
k_4 (min^{-1}) =	64	6.40×10^{-2}	0.256	1.02	4.00	16.0
	16	1.60×10^{-2}	6.40×10^{-2}	0.256	1.00	4.00
	4	4.00×10^{-3}	1.60×10^{-2}	6.40×10^{-2}	0.250	1.00
	1	1.00×10^{-3}	4.00×10^{-3}	1.60×10^{-2}	6.25×10^{-2}	0.250
	0.25	2.50×10^{-4}	1.00×10^{-3}	4.00×10^{-3}	1.56×10^{-2}	6.25×10^{-2}
	0.064	6.40×10^{-5}	2.56×10^{-4}	1.02×10^{-3}	4.00×10^{-3}	1.60×10^{-2}
	0.016	1.60×10^{-5}	6.40×10^{-5}	2.56×10^{-4}	1.00×10^{-3}	4.00×10^{-3}
$p(k_2/k_1)$ =		5.40	6.00	6.60	7.19	7.80
pK_D =		8.40	8.40	8.40	8.40	8.40
pK_D* =		8.40	8.40	8.40	8.42	8.49
	k_3 (min^{-1})					
$^{app}pK_D$* =	64	7.88	7.89	7.89	7.90	7.91
	16	7.82	7.87	7.89	7.90	7.91
	4	7.64	7.81	7.87	7.89	7.91
	1	7.27	7.63	7.81	7.88	7.90
	0.25	6.75	7.26	7.63	7.82	7.89
	0.064	6.20	6.77	7.29	7.66	7.85
	0.016	5.72	6.31	6.89	7.41	7.70

C) Saturation binding curves for L variants A to D after increasing incubation times.

Figure 1 (below) shows that all saturation binding curves experience a gradual time-dependent shift to the left and eventually a steepening (i.e. decline of n_H till unity). When equilibrium binding is finally reached, the ligand concentration at which 50 % receptors are occupied equals K_D*. The saturation curves at selected time points are depicted at the left side of each panel. Simulated curves are subjected to nonlinear regression analysis according to a variable slope sigmoidal dose-response curve paradigm (in Prism 4 by GraphPad Software Inc., San Diego, CA). In the mid, the $^{app}pK_D$* values of such curves are plotted as a function of the incubation time (in logarithmic scale) and, at the right side, the n_H values are also plotted as a function of the incubation time.

Figure 1.

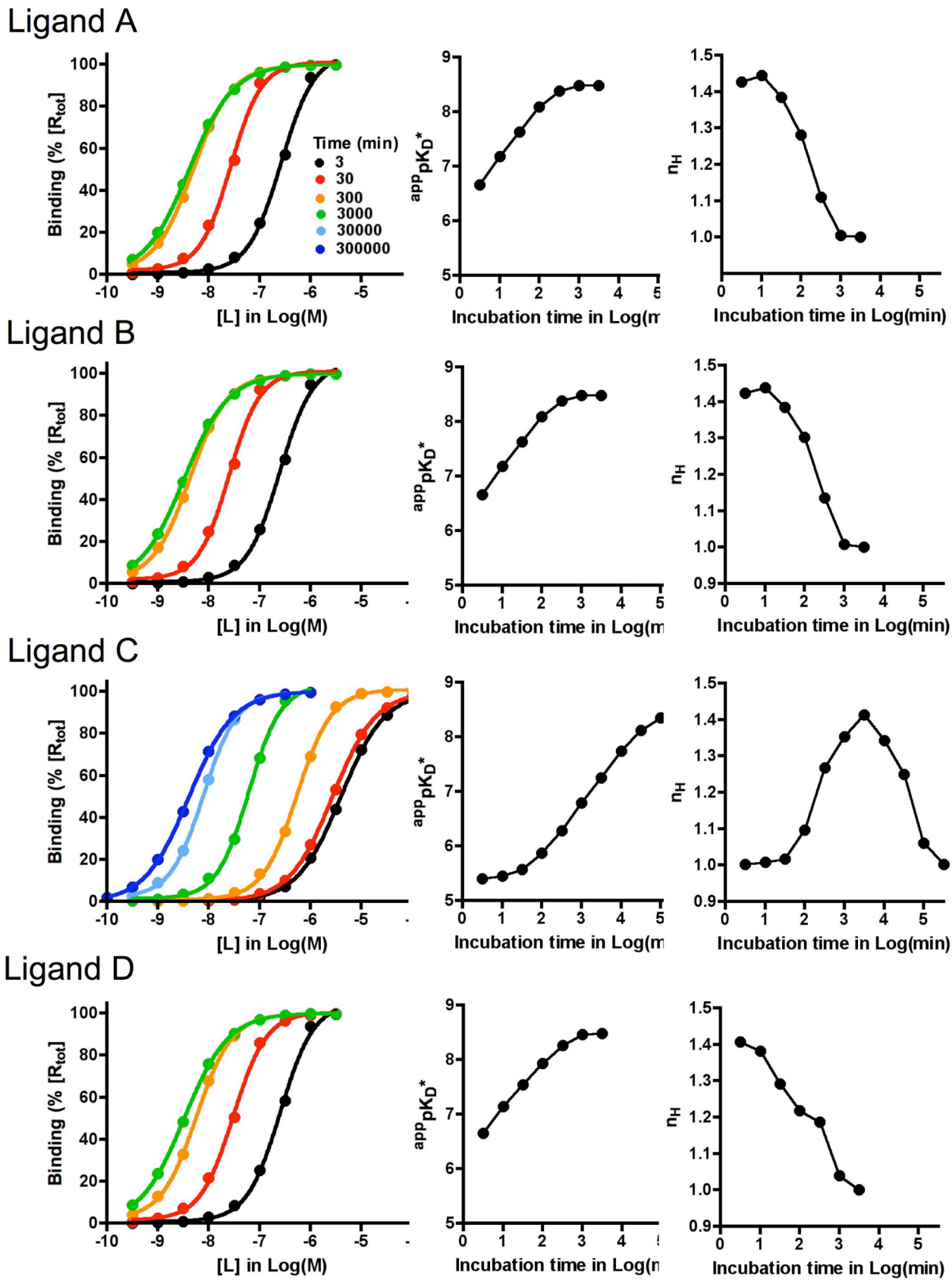
Ligand A
Binding (% [Rtot])
[L] in Log(M)
Time (min)
3
30
300
3000
30000
300000
appKD*
Incubation time in Log(m
nH
Incubation time in Log(min)
Ligand B
Binding (% [Rtot])
[L] in Log(M)
appKD*
Incubation time in Log(m
nH
Incubation time in Log(min)
Ligand C
Binding (% [Rtot])
[L] in Log(M)
appKD*
Incubation time in Log(m
nH
Incubation time in Log(min)
Ligand D
Binding (% [Rtot])
[L] in Log(M)
appKD*
Incubation time in Log(m
nH
Incubation time in Log(min)

Figure 2 (below) shows that, when ligand C occupies > 99 % of the receptors, [RL] only represents a sizable portion of the binding (i.e. [RL] + [R'L]) early on and then gradually drops to become a negligible portion of the binding after 300 min incubation or longer. At equilibrium, [RL] only represents 0.1 % the binding (since k_3/k_4 = 1000). This implies that a two-step induced-fit- type binding mechanism could have been easily overlooked when exploring the insurmountable behavior and association binding of ligands like C after very long (pre)incubation.

Figure 2

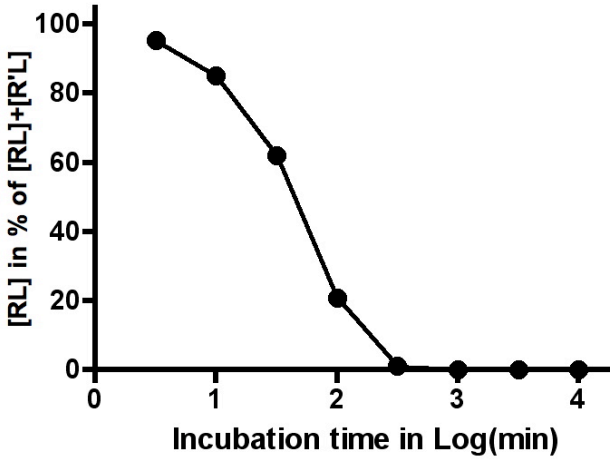

D) Insurmountable behavior of L variants A to D.

"Organ-bath"-type functional assays may hint at an induced fit binding mechanism. Those assays comprise preincubating the receptors with antagonist and then briefly challenging with agonist (Leff and Martin, G.R., 1986). Fast-dissociating competitive antagonists may only shift the agonist concentration- response curves to the right. This behavior is denoted as "surmountable". Other antagonists dissociate more slowly and may also decrease the maximal response if a new mass-action equilibrium is not yet resumed when the response is measured (Vauquelin et al., 2002a,b; Kenakin et al., 2006). When L binds according to an induced-fit mechanism, comparable quantities of fast dissociating RL and more stable R'L complexes may be present at the onset of the incubation with agonist. Yet, conditions apply for the appropriate quantification of this [R'L]/[RL] ratio in terms of insurmountable and surmountable binding. Besides the absence of (or only minor) cellular amplification of the signal (such as in the simulations presented in the main article and hereafter), the incubation with the agonist has to be long enough to allow near- complete dissociation of RL and yet short enough to prevent perceptible dissociation of R'L. (Vauquelin et al., 2002a,b). This implies that

the dissociation of RL has to be substantially faster than the dissociation of R'L. In this respect, the simulations shown in Figure 3 reveal that ligand C complies best with those criteria.

For Figure 3, receptors are incubated for 60 min with a receptor near-saturating concentration of antagonist (0.1 μM for A, B and D and 30 μM for C) and then incubated for increasing time periods with agonist (kon = $1x10^7$ $M^{-1}.min^{-1}$, koff = 1 min^{-1}) after which the response (here proportional to receptor occupancy by the agonist) is measured. Differential equations that are relevant to these simulations are provided in Table 1. Agonist concentration-response curves are shown at the left side of each panel and the amount RL and R'L complexes are shown as a function of the incubation time with agonist at the right side of each panel. After preincubation with ligands A, B and D, the maximal response of the agonist increases gradually with time as a result of the combined decline of RL and R'L. As expected, RL declines faster as R'L and, similar to the dissociation curves in Figure 3b of the main article, there is even a transient increase of R'L for ligand D. Although less perceptible at first sight, the agonist concentration-response curve also shifts to the right when the incubation time increases. For ligand C, the maximal response of the agonist does not perceptibly vary with the incubation time due to the persistence of R'L. Here again, the agonist concentration-response curve will gradually shift to the right when the incubation time increases.

For Figure 4, simulated agonist concentration-response curves after preincubation with ligand C are subjected to nonlinear regression analysis according to a variable slope sigmoidal dose-response paradigm (in Prism 4 by GraphPad Software Inc., San Diego, CA). Log(A_2) values of C are then calculated based on the shift between the EC_{50} values of the curves after antagonist pretreatment (denoted as $EC_{50}2$) and the value of the control curve (i.e. in the absence of antagonist, denoted as $EC_{50}1$) according to the method of Arunlakshana and Schild (1959). In short: such as shown in the left and mid panel of Figure 4, the dotted lines with a slope factor of 1 allow the conversion of Log(($EC_{50}2/EC_{50}1$) - 1) into Log(A_2) values that correspond to the intercepts with the abscissa.

In the left panel of Figure 4, increasing the incubation time with agonist decreases the Log(A_2) values of ligand C. On the other hand, the Log(A_2) values remain steady and very close to Log(k_2/k_1) when increasing the concentration of C (mid panel) or extending the preincubation time (right panel). Data are based on the simulations shown in the right panel on Figure 3, Figure 2b of the main article and Figure 2c of the main article, respectively.

Figure 3.

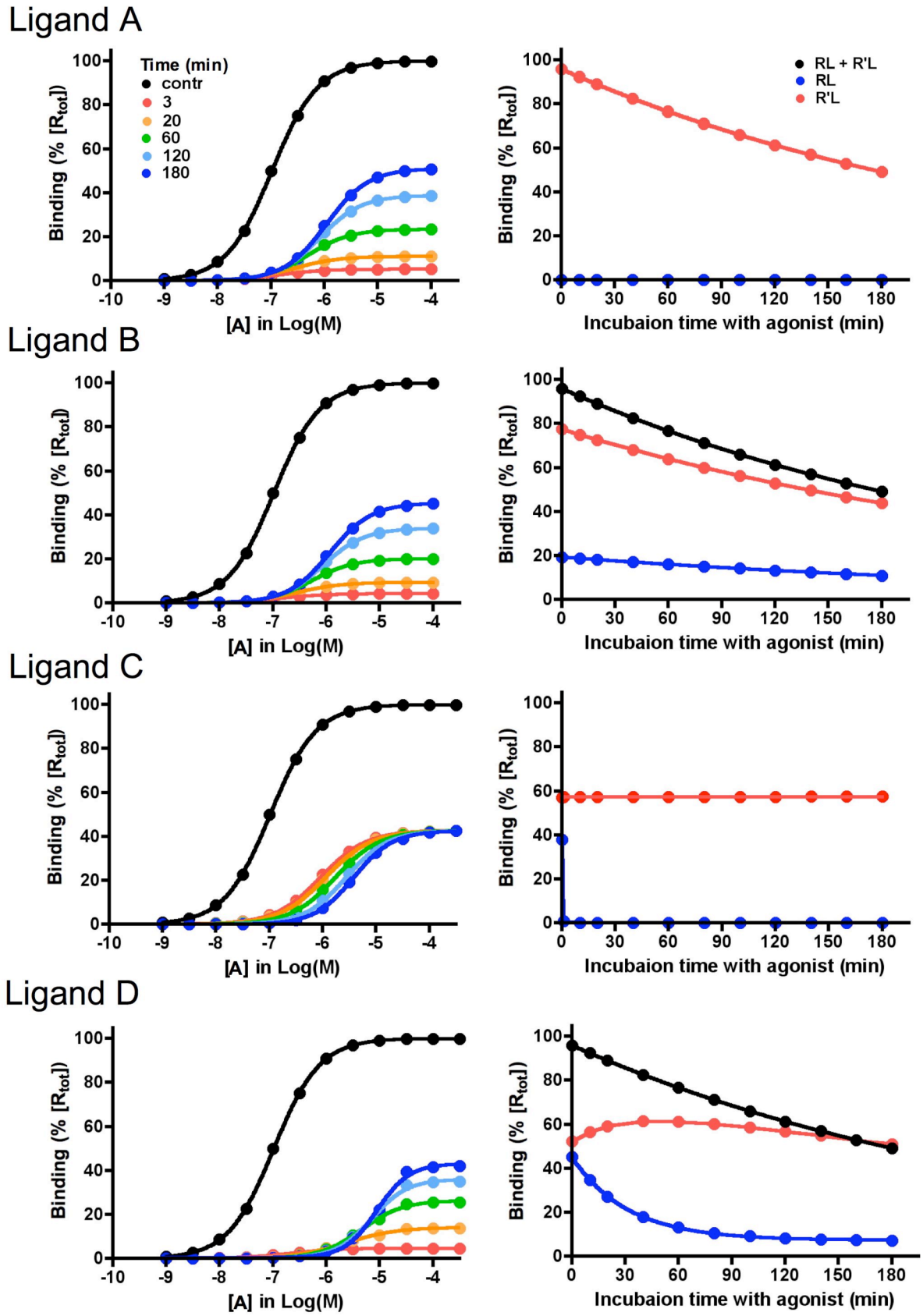
Ligand A
Time (min)
contr
3
20
60
120
180
Binding (% [Rtot])
[A] in Log(M)
RL + R'L
RL
R'L
Incubaion time with agonist (min)
Ligand B
Ligand C
Ligand D

Figure 4.

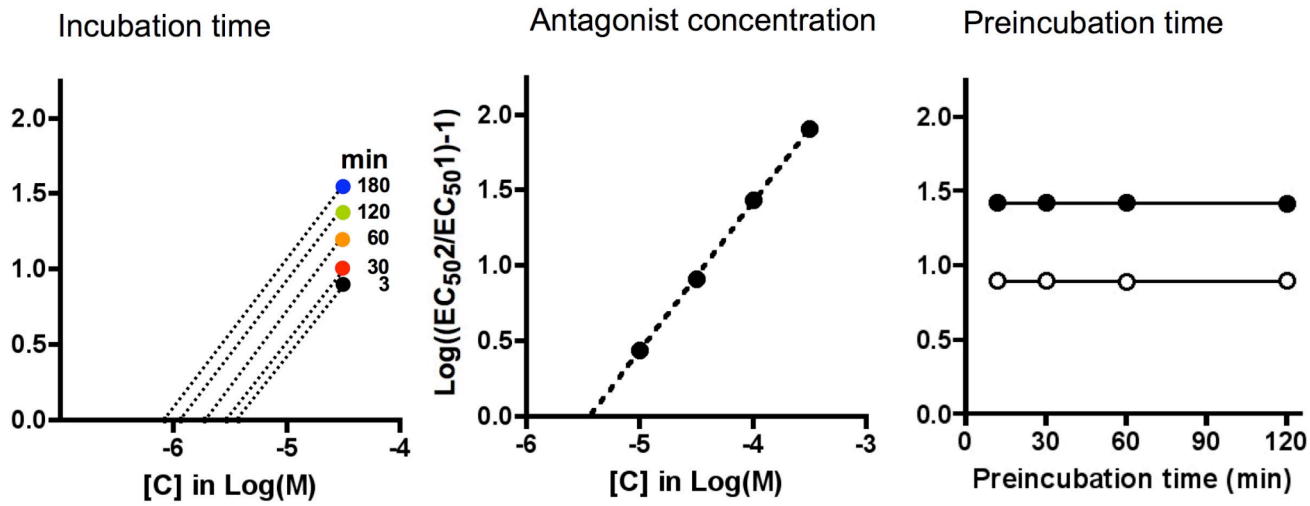

E) References

Arunlakshana, O Schild HO (1959). Some quantitative uses of drug antagonists. *Br J Pharmacol Chemother* **14**: p. 48-58.

Hoare SRJ (2007). Allosteric modulators of class B G-protein-coupled receptors. *Curr Neuropharmacol* **5**: 168-179.

Kenakin, T, Jenkinson, S, Watson, C. (2006). Determining the potency and molecular mechanism of action of insurmountable antagonists. *J Pharm Exp Ther* **319**: 710-723.

Leff P, Martin GR (1986). Peripheral 5-HT_2-like receptors. Can they be classified with the available antagonists? *Brit J Pharmacol* **88**: 585-593.

Strickland S, Palmer G, Massey V (1975). Determination of dissociation constants and specific rate constants of enzyme-substrate (or protein-ligand) interactions from rapid reaction kinetic data. *J Biol Chem* **250**: 4048-4052.

Tummino PJ, Copeland RA (2008). Residence time of receptor- ligand complexes and its effect on biological function. *Biochemistry* 47: 5481-5492.

Vauquelin G, Charlton S (2013). Exploring avidity, understanding the potential gains in functional affinity and target residence time of bivalent and heterobivalent ligands. *Brit J Pharmacol* **168**: 1771-1785.

Vauquelin G, Morsing P, Fierens FLP, De Backer J-P, Vanderheyden PML (2001a). A two-state receptor model for the interaction between angiotensin II AT_1 receptors and their non-peptide antagonists. *Biochem Pharmacol* **61**: 277-284.

Vauquelin G, Van Liefde I, Vanderheyden P (2002a). Models and methods for studying insurmountable antagonism. *Trends Pharmacol Sci* **23**: 514-518.

Vauquelin G, Van Liefde I, Birzbier BB, Vanderheyden PML (2002b). New insights in insurmountable antagonism. *Fund Clin Pharmacol* **16**: 263-272.

Vauquelin G, Hall D, Charlton P (2015). "Partial" competition of heterobivalent ligand binding may be mistaken for allosteric interactions: A comparison of different target interaction models. *Brit J Pharmacol* doi 172, 2300-2315.